

Site-Specific Protein Labeling with Fluorophores as a Tool To Monitor Protein Turnover

Journal Article**Author(s):**

Mideksa, Yonatan G.; Fottner, Maximilian; Braus, Sebastian; Weiß, Caroline A.M.; Nguyen, Tuan-Anh; Meier, Susanne; Lang, Kathrin; Feige, Matthias J.

Publication date:

2020-07-01

Permanent link:

<https://doi.org/10.3929/ethz-b-000424422>

Rights / license:

[Creative Commons Attribution-NonCommercial 4.0 International](#)

Originally published in:

ChemBioChem 21(13), <https://doi.org/10.1002/cbic.201900651>

Site-Specific Protein Labeling with Fluorophores as a Tool To Monitor Protein Turnover

Yonatan G. Mideksa,^[a] Maximilian Fottner,^[a] Sebastian Braus,^[a, c] Caroline A. M. Weiß,^[a] Tuan-Anh Nguyen,^[a] Susanne Meier,^[a] Kathrin Lang,^[a, b] and Matthias J. Feige*^[a, b]

Proteins that terminally fail to acquire their native structure are detected and degraded by cellular quality control systems. Insights into cellular protein quality control are key to a better understanding of how cells establish and maintain the integrity of their proteome and of how failures in these processes cause human disease. Here we have used genetic code expansion and fast bio-orthogonal reactions to monitor protein turnover in mammalian cells through a fluorescence-based assay. We have used immune signaling molecules (interleukins) as model

substrates and shown that our approach preserves normal cellular quality control, assembly processes, and protein functionality and works for different proteins and fluorophores. We have further extended our approach to a pulse-chase type of assay that can provide kinetic insights into cellular protein behavior. Taken together, this study establishes a minimally invasive method to investigate protein turnover in cells as a key determinant of cellular homeostasis.

Introduction

In order to become biologically active, most proteins have to adopt defined three-dimensional structures: that is, to fold. Protein folding is among the most fundamental processes of self-organization in living systems and at the same time is highly complex: in a correctly structured protein, thousands of atoms each adopt a well-defined position in space.^[1] Accordingly, cells have developed a comprehensive machinery of protein folding helpers, molecular chaperones, to aid protein folding—but also to scrutinize its success and to degrade proteins that do not achieve their native structure.^[2] Failures in these processes give rise to protein misfolding disorders such as Parkinson's or Alzheimer's diseases.^[3]


In a mammalian cell, the endoplasmic reticulum (ER) is specialized in the production and folding of membrane and secreted proteins.^[4] These proteins mediate cellular communication, transport processes, and coordinated development, and in total make up more than one third of a typical mammalian proteome.^[5] As such, the ER can be considered a bona fide protein-folding factory in the cell, which also sets the standards that determine whether a protein shall be transported to the cell surface or shall be degraded if it fails to fold.^[6] This process is termed ER quality control (ERQC). Generally, proteins that fail to acquire their native structures in the ER are eliminated in a process called ER-associated degradation (ERAD).^[7] ERAD includes recognition of misfolded proteins in the ER, their retro-translocation back to the cytosol, ubiquitination, and subsequent degradation by the major proteolytic machinery of the cell, the proteasome.^[7,8] Its fundamental role in cell biology, and its immediate involvement in human disease, have spurred great interest in understanding the molecular basis of ERAD,^[9] as well as in developing techniques to monitor this process.^[10–12]


The site-specific incorporation of unnatural amino acids (UAAs) through genetic code expansion and their subsequent chemoselective labeling with fluorescent probes might present an ideal tool with which to monitor ERAD and protein turnover in general.^[13] Recent years have seen tremendous progress in the development of rapid and selective bio-orthogonal reactions such as inverse-electron-demand Diels–Alder cycloaddition (IEDDAC) between strained dienophiles and tetrazines.^[14–17] Unnatural amino acids bearing strained alkene or alkyne motifs, such as bicyclo[6.1.0]nonyne (BCNK)^[16,18] and *trans*-cyclooctene (TCOK),^[16,17] have been incorporated site-specifically into proteins in *Escherichia coli* and in mammalian cells with the aid of specific and orthogonal pyrrolysyl-tRNA synthetases.

[a] Y. G. Mideksa, M. Fottner, S. Braus, C. A. M. Weiß, T.-A. Nguyen, Dr. S. Meier, Prof. Dr. K. Lang, Prof. Dr. M. J. Feige
Center for Integrated Protein Science Munich (CIPSM) at the Department of Chemistry
Technical University of Munich
Lichtenbergstrasse 4, 85748 Garching (Germany)
E-mail: matthias.feige@tum.de

[b] Prof. Dr. K. Lang, Prof. Dr. M. J. Feige
Institute for Advanced Study, Technical University of Munich
Lichtenbergstr.2a, 85748 Garching (Germany)

[c] S. Braus
Current address: Institute of Molecular Biology and Biophysics
ETH Zürich
8093 Zürich (Switzerland)

 Supporting information and the ORCID identification numbers for the authors of this article can be found under <https://doi.org/10.1002/cbic.201900651>.

 © 2020 The Authors. Published by Wiley-VCH Verlag GmbH & Co. KGaA. This is an open access article under the terms of the Creative Commons Attribution Non-Commercial License, which permits use, distribution and reproduction in any medium, provided the original work is properly cited and is not used for commercial purposes.

tase (PylRS/trNA_{CUA}) pairs. Rapid iEDDAC with tetrazine fluorophore conjugates allows the site-specific and selective labeling of proteins in living cells with a diverse range of fluorophores,^[16,17] and has been used for imaging of cell-surface and intracellular proteins,^[19–23] as well as to control enzyme activities in cells.^[24]

Here we have made use of this potential and developed a fluorescence-based assay for monitoring protein turnover in mammalian cells. We have site-specifically incorporated BCNK^[16,18] into low-abundance mammalian proteins by using an efficient PylRS variant, which allows for fast and selective protein labeling with tetrazine-fluorophore conjugates. This extends the arsenal of methods that have been developed in recent years to monitor protein turnover in cells^[25–27] by a fluorescence-based approach that relies on rapid bio-orthogonal reactions. As model substrates, we have used members of the human interleukin 12 (IL-12) family.^[28,29] Interleukins are key signaling molecules in our immune system and, as such, understanding of their biogenesis and degradation is of great interest. Like other secreted proteins, interleukins are produced in the ER, each IL-12 family member being a heterodimeric protein made up of an α and a β subunit.^[28,29] It has recently been shown that both IL-12 α and IL-23 α fail to fold in the absence of their β subunits and are thus rapidly degraded,^[30–32] providing native clients of ER quality control. Our data show that incorporation of BCNK and site-specific fluorophore labeling of IL-12 α and IL-23 α preserves their normal biogenesis processes and provides an ideal tool with which to monitor protein turnover in mammalian cells.

Results and Discussion

Unnatural amino acids can be incorporated into interleukin subunits while maintaining their wild-type behavior

A major advantage of genetic code expansion is that it offers the capability to label any position within a polypeptide sequence with only minimal modifications to the protein under scrutiny. Here we have used a selective and highly efficient PylRS variant (Y271G, C313V, *Methanosarcina barkeri* numbering, dubbed BCNKRS, Figure S1A in the Supporting Information)^[33] for expression of low-abundance interleukins bearing BCNK at defined positions. Beginning with the α subunit of IL-12 (IL-12 α , Figure 1A), we searched for a suitable position at which to introduce BCNK (Figure 1B). Criteria were complete solvent-exposure in the native heterodimeric IL-12 structure as well as no predicted interference with IL-12 β heterodimerization.^[34] Asp31 (D31) and Gln57 (Q57) fulfilled these criteria (Figure 1A). By using BCNKRS and BCNK we could achieve significant expression for the IL-12 α constructs in which D31 or Q57 were replaced by an amber stop codon (D31* or Q57*, respectively). Expression did not vary significantly between 0.1 and 1 mM BCNK (Figure S1B). At 0.25 mM BCNK, expression levels of IL-12 α D31BCNK were still (34 ± 4)% (mean ± SEM) and for IL-12 α Q57BCNK (54 ± 6)% (mean ± SEM) of those observed for the wild-type (wt) protein (Figure 1C).

On the basis of these findings, we next assessed wild-type (wt)-like behavior of the BCNK-bearing IL-12 α variants in terms of ER quality control. IL-12 α is retained in cells in isolation and forms incorrect disulfide bonds. Only the co-expression of IL-12 β induces correct folding.^[30] IL-12 α D31BCNK showed wt behavior and was retained in cells in isolation and only secreted efficiently upon co-expression of IL-12 β , including modification of its glycan residues in the Golgi,^[30] thus implying that ERQC works properly on the modified protein (Figure 1D). The same behavior was observed for IL-12 α Q57BCNK, thus corroborating the minimally invasive character of BCNK incorporation (Figure 1E). By using interleukin-responsive reporter cell lines we were furthermore able to show that IL-12 containing BCNK was also biologically active, even when fluorophore was added, thus implying proper folding in the presence of BCNK and fluorophore (Figure S1C).

Lastly, by extending our approach to IL-23, another IL-12 family member prominently involved in autoimmune reactions and tumor development,^[29,35,36] we found that BCNK could also be incorporated site-specifically into this protein with preservation of normal ERQC³¹ and biological activity (Figure S1D–G).

Rapid bio-orthogonal fluorescence labeling of interleukin subunits

Having established efficient incorporation of BCNK into IL-12 α and IL-23 α with preservation of wt-like behavior, we proceeded to fluorescent labeling of BCNK-modified proteins. We focused on IL-12 α for a detailed characterization. Our first goal was to establish optimal labeling conditions. By using either tetramethylrhodamine-tetrazine (TAMRA-tetrazine, Figure S2A–F) or silicon rhodamine-tetrazine (SiR-tetrazine, Figure 2A–D) we could efficiently label IL-12 α containing BCNK in living cells at fluorophore concentrations from 100–400 nM (Figure 2A–C) even after as little as 5 min (Figure 2D), with increasing labeling efficiencies being observed after longer labeling times in the case of TAMRA-tetrazine (Figure S2D–F) and very rapid labeling in that of SiR-tetrazine (Figure S2, G and H).

Bio-orthogonal fluorescence labeling allows protein turnover to be monitored

Taken together, these characteristics (wt-like behavior combined with rapid and efficient labeling) provided us with an excellent tool with which to monitor protein turnover. To this end, we first labeled IL-12 α containing BCNK at position 31 or 57 with SiR-tetrazine or BODIPY-tetramethylrhodamine-tetrazine (B-TMR-tetrazine), respectively, for 15 min. Subsequently, we washed out the fluorophore and added an excess of free BCNK to quench all tetrazine fluorophore and at the same time maintain translation of the target protein IL-12 α . Hence, this approach should allow for observation of selective degradation of the fluorescently labeled protein pool without disturbing global translation in the cell (schematic in Figure 3A, B). Because an UAA was used instead of radioactive amino acids to follow protein degradation in classical pulse-chase experiments, we termed this approach *uChase*. As expected, we ob-

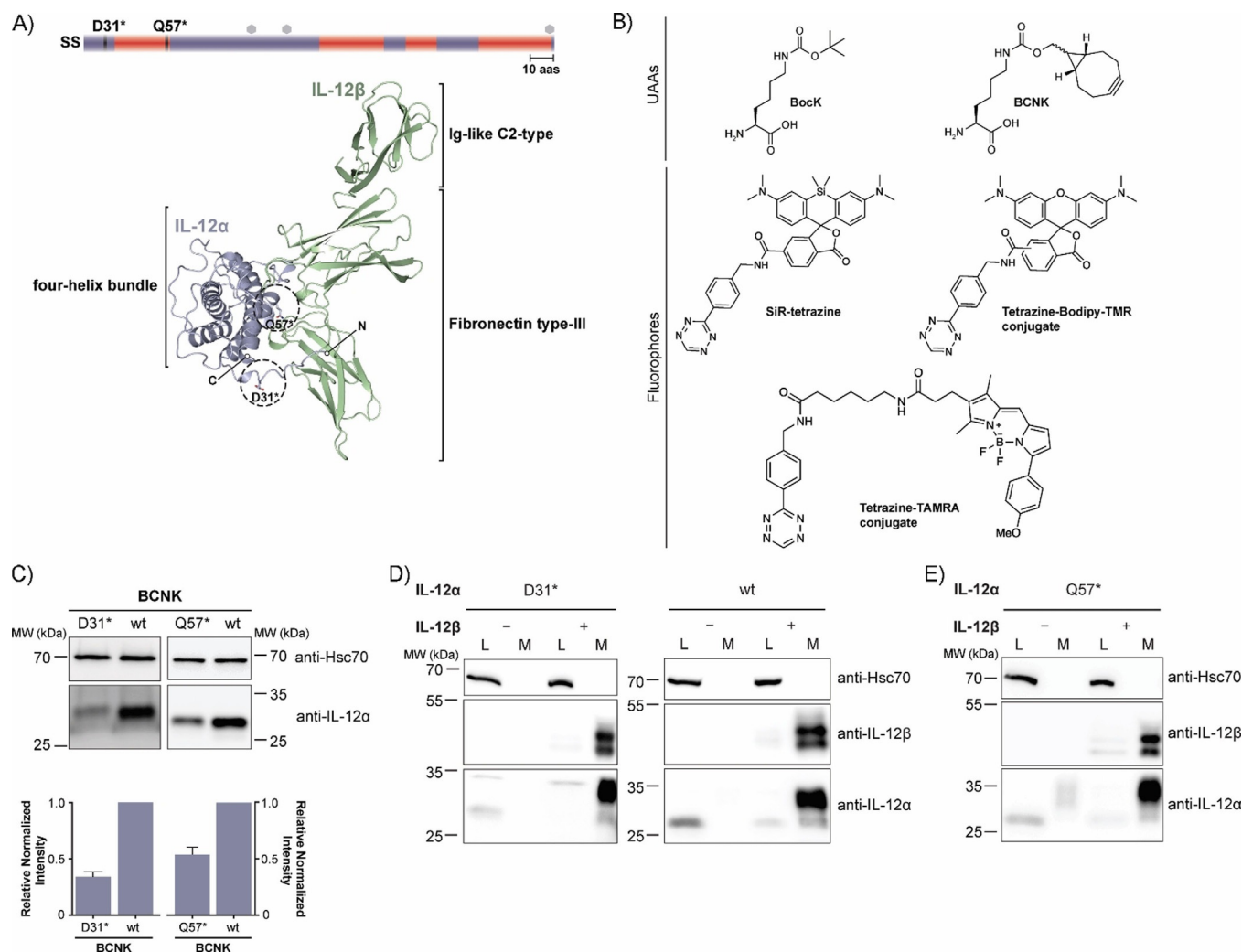


Figure 1. Noncanonical amino acid incorporation into IL-12 in mammalian cells. A) Top: Schematic representation of the IL-12 α secondary structure (SS = signal sequence, red = α -helices, mauve = loops, hexagons = predicted glycosylation sites, 10 aas = 10 amino acids). Positions of amber codons (D31 and Q57) are indicated. Bottom: PDB structure of heterodimeric IL-12 (PDB ID: 3HMx. Missing residues were modeled); N and C termini are indicated for IL-12 α . The positions selected for UAA incorporation into IL-12 α are marked with dashed circles. B) Unnatural amino acids (UAAs) and fluorophores used in this study. C) Top: Immunoblots of HEK-293T cells expressing the BCNKR/S/PyIT pair and IL-12 α ^{D31TAG} or IL-12 α ^{Q57TAG} (abbreviated as D31* or Q57*, respectively) in the presence of BCNK. Bottom: Expression of IL-12 α D31BCNK and IL-12 α Q57BCNK relative to wild-type IL-12 α was quantified from $N=6$ (D31BCNK) or $N=3$ (Q57BCNK) immunoblots (mean \pm SEM), respectively. Samples were normalized for Hsc70 levels. D) IL-12 α D31BCNK was tested for assembly-induced secretion upon co-expression of IL-12 β . HEK293T cells were co-transfected with the indicated constructs in the presence of BCNK and samples were analyzed by immunoblotting. An increase in molecular weight upon secretion can be attributed to modification of IL-12 α glycans in the Golgi and IL-12 β populates two different glycospecies.^[30] L = lysate, M = medium, wt = wild-type control. E) As in (D) but for IL-12 α Q57BCNK.

served decreasing IL-12 α fluorescence for D31BCNK and Q57BCNK in *uChase* experiments (Figure 3C, D top). Notably, this analysis was based on whole-cell lysates, and thus does not depend on any downstream enrichment steps and also works for interleukins as proteins expressed at low levels (Figure S3A–D). Furthermore, the assay was compatible with use either of SiR-tetrazine (Figure 3C) or of B-TMR-tetrazine (Figure 3D) as fluorophore-tetrazine conjugates to label IL-12 α . Starting from steady-state, immunoblots revealed that the overall level of IL-12 α essentially remained constant over the time of the chase, as initially hypothesized (Figure 3C, D, middle). The slight increase in protein levels can likely be attributed to the necessary washing steps before labeling, which were performed in the absence of BCNK. This will deplete cells

of BCNK during these steps and thus lead to degradation of a small amount of IL-12 α before the BCNK excess is added and translation from Amber codon-containing transcripts can resume. Consistent with previous studies,^[30,32] the half-life for IL-12 α degradation determined by our new *uChase* assay was (2.5 \pm 0.3) h (with use of D31* and SiR) and (2.2 \pm 0.2) h (with use of Q57* and B-TMR; Figure 3C, D, bottom), thus showing that labeling position and choice of fluorophore did not significantly affect the outcome of our experiment. Furthermore, neither BCNK incorporation nor SiR labeling (Figure S4A and B) significantly changed the half-life of IL-12 α in cycloheximide (CHX) chases, underscoring the minimally invasive character of our approach and establishing *uChase* as a way to monitor protein degradation. Two assays were performed to confirm

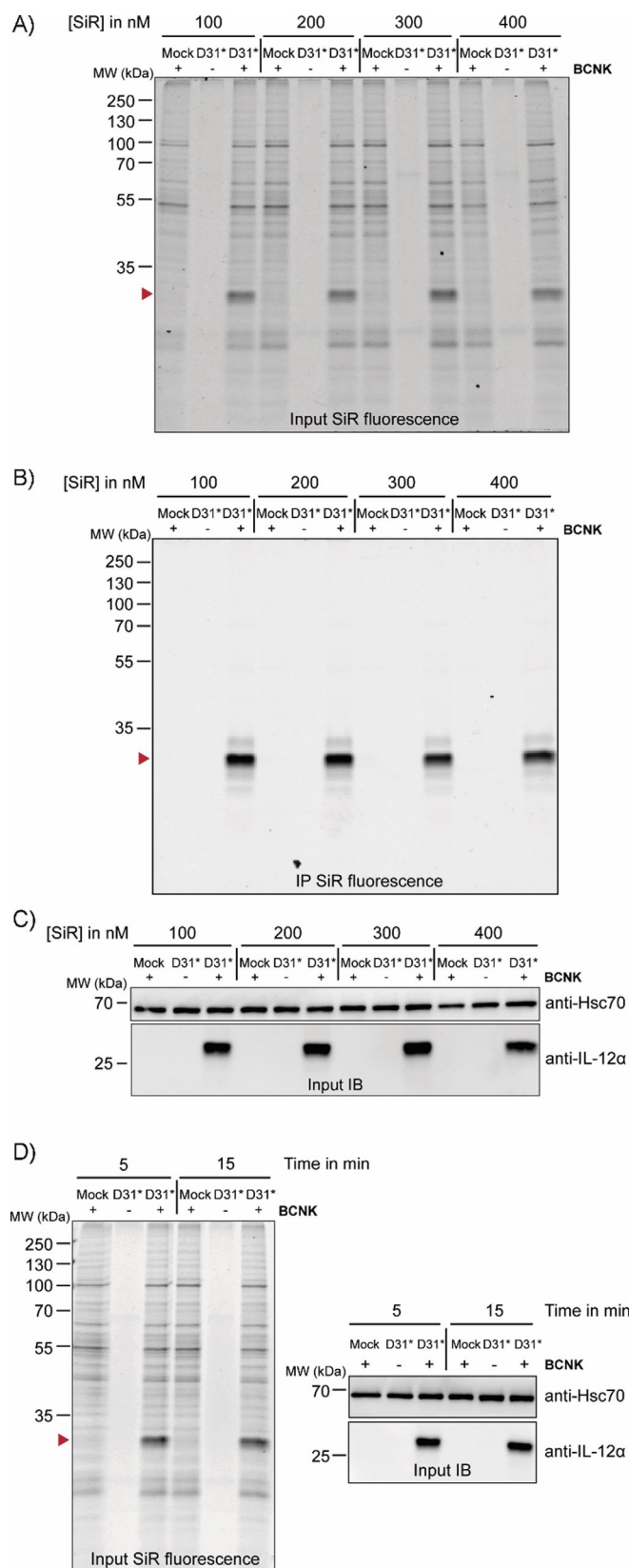


Figure 2. Bio-orthogonal fluorescent labeling of BCNK-modified IL-12 α is fast and efficient. A)–C) Cells expressing IL-12 α D31* constructs at 0.25 mM BCNK were treated with the indicated concentrations of SiR-tetrazine fluorophore for 15 min and analyzed by A) in-gel fluorescence of lysates (IL-12 α D31BCNK is marked with a red arrowhead), B) after immunoprecipitation (IP), and C) by immunoblotting (IB). The + and – lanes refer to the presence or absence of BCNK. SiR-tetrazine fluorophore was present in all samples. D) Left: Representative gel for a reaction time course between 400 nM SiR-tetrazine and IL-12 α D31BCNK analyzed by in-gel fluorescence. Right: Cell lysates were additionally analyzed by immunoblotting.

(Figure 3E). As a further test we used a dominant negative mutant of the ERAD E3 ubiquitin ligase Hrd1 (Hrd1^{C[291]S}).^[37] This mutant decelerated degradation of IL-12 α in CHX chases (Figure S4C) and to a similar extent degradation of B-TMR-labeled IL-12 α Q57BCNK in *uChase* assays (Figure S4D and E), thus further validating our assay as a tool with which to monitor ERAD.

To demonstrate a more general applicability of our approach we additionally analyzed IL-23 α L150BCNK. For this protein, degradation occurred with a half-life of less than 2 h, and was again not significantly affected by incorporation of BCNK (Figure S4F). When IL-23 α L150BCNK was labeled with B-TMR, our *uChase* approach again yielded a half-life similar to those determined by CHX chases^[31] (Figure S4F and G), thus showing that our approach can also be extended to other proteins with more rapid cellular turnover.

Development of a fluorescence-based pulse-chase assay

So far, our approach was similar to classical CHX chases because we started from a steady-state pool of proteins, and then monitored their degradation, yet without globally inhibiting translation. Ideally, as possible with radioactive labeling^[10] and recently developed techniques for cytoplasmic proteins,^[13] one would like to label the protein of interest produced within a defined time interval, and then monitor its cellular fate. This, for example, would allow analysis of transport processes and post-translational modifications such as changes in glycosylation with temporal resolution.^[38] To assess if such an approach (Figure 4A) was in reach with our setup, we first analyzed how long BCNK needed to be added to cells in order for expression of IL-12 α Q57BCNK to be observed. Even after as little as 30 min we observed sufficient expression of IL-12 α Q57BCNK for detection by immunoblotting (Figure 4B, C). Addition of BCNK for a 1 h pulse, labeling with B-TMR for 15 min, and subsequent addition of a BCNK excess (chase) allowed us to monitor protein degradation of IL-12 α Q57BCNK produced within this 1 h time window (Figure 4A, D, E).

In these experiments, a half-life of (1.1 ± 0.1) h (from input samples) was observed for IL-12 α Q57BCNK. This might suggest that on a molecular level an IL-12 α pool produced within only a 1 h pulse period differs to some extent from the steady-state pool. It should be noted that IL-12 α forms different redox species in cells, including homodimers.^[30] Their formation has not been kinetically analyzed yet but might impact degradation and give rise to this behavior. This further highlights the

that our assay monitored ERAD. Degradation of IL-12 α in our *uChase* assay was mediated by the proteasome as expected for an ERAD substrate, because it could be inhibited by MG132

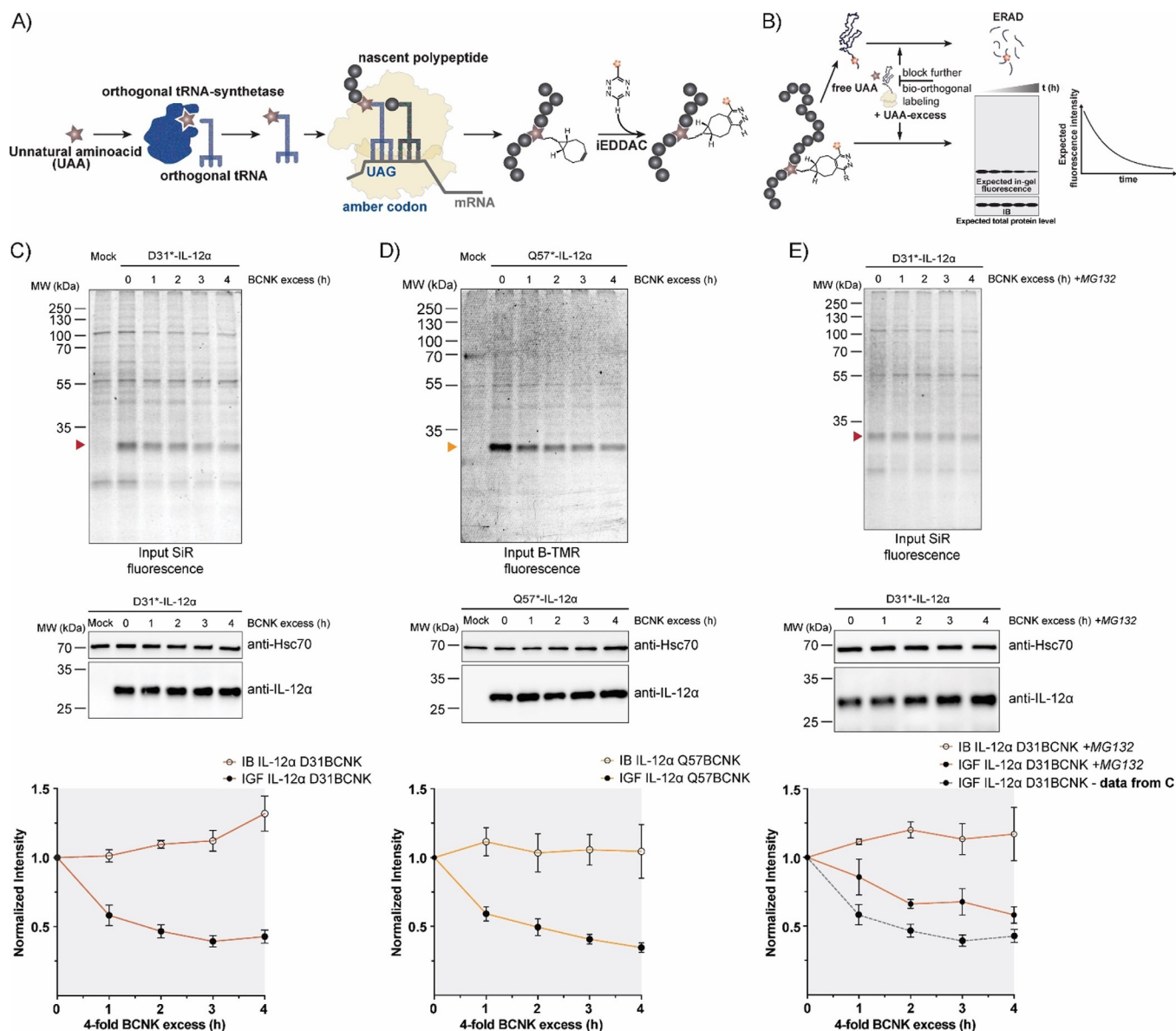


Figure 3. Protein turnover monitored by the *uChase* approach. A) Workflow of in-cellulo bio-orthogonal labeling. During translation, an in-frame TAG stop codon is suppressed by an evolved orthogonal tRNA-synthetase/tRNA pair carrying the UAA. Next, the UAA can be labeled chemoselectively with a suitable probe, such as a fluorophore. B) *uChase* as a tool for monitoring protein degradation. To monitor protein removal rates (e.g., through ERAD), free UAA is washed out before the labeling reaction. Then, cells are treated with an excess of free UAA for a desired time interval to block any further bio-orthogonal labeling of newly synthesized proteins without altering the protein biogenesis machinery. The protein half-life can be measured from intensity plots quantified from in-gel fluorescence (IGF) intensities of cell lysates. Total protein levels, as measured by immunoblotting (IB), are expected to remain constant. C) Top: Time course of fluorescence decrease for labeled IL-12 α D31BCNK; 0.25 mM BCNK and 400 nM SiR-tetrazine fluorophore (15 min labeling) were used, followed by incubation with a fourfold excess of BCNK for the indicated time points and analyzed by in-gel fluorescence. Middle: Total protein levels of IL-12 α D31BCNK were analyzed by immunoblotting. Bottom: The graph shows quantifications from in-gel fluorescence and immunoblotting data, $N=5$ (mean \pm SEM). The intensity of the 0 h time point was set to 1. IB: immunoblotting. IGF: in-gel fluorescence. D) The same analyses as shown in (C), but for the IL-12 α Q57BCNK variant labeled with B-TMR [$N=4$ (mean \pm SEM)]. E) IL-12 α D31BCNK degradation was inhibited by the proteasomal inhibitor MG132 and the effect was analyzed by use of the *uChase* assay as in (C), $N=4$ (mean \pm SEM). A dotted gray line (bottom panel) shows IGF data from (C), (bottom panel) as a reference.

importance of pulse-chase types of approaches. Because we were starting from a small pool of IL-12 α Q57BCNK (Figure 4B, C), the decrease in the pool of fluorescently labeled protein (Figure 4D, E) was accompanied by an increase in overall IL-12 α Q57BCNK levels during the 4 h chase. This is due to the fact that BCNK was present during the chase that allows for

the synthesis of new, nonfluorescent IL-12 α Q57BCNK molecules (Figure 4F). Taken together, these data show that a pulse-chase approach is also possible with *uChase*, which opens up further future fluorescence-based applications.

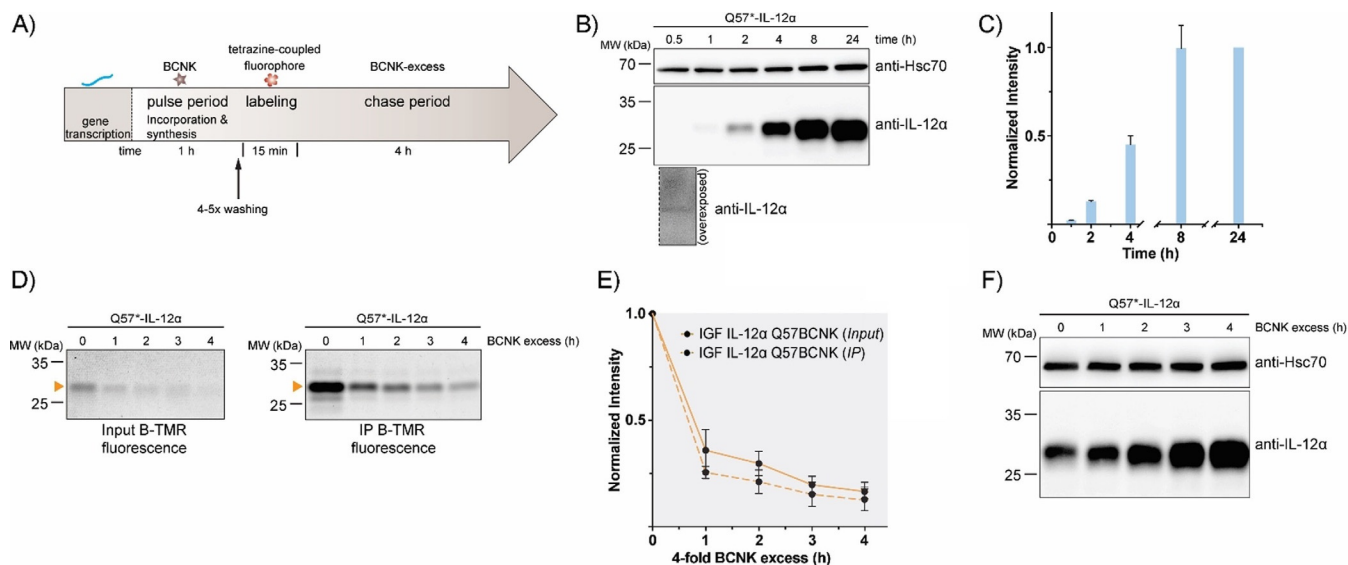


Figure 4. Establishment of a *uChase*-based pulse-chase assay. **A)** Illustration of a *uPulse-chase* experiment. BCNK addition for a defined time interval (pulse period) allows protein synthesis from mRNA present to occur. After washing out of free BCNK and brief labeling with a tetrazine-coupled fluorophore, a chase period follows (as described Figure 3 B). **B)** Representative immunoblots showing expression levels of IL-12 α Q57BCNK after different time intervals of the 0.25 mM BCNK pulse. An overexposure for the 30 min time point is shown below the blot. **C)** The graph shows a quantification from immunoblots; $N = 4$ (mean \pm SEM). Samples were normalized for Hsc70 levels. The intensity of the 24 h time point was set to 1. **D)–F)** Following the schematic in (A), IL-12 α Q57BCNK degradation was followed by a *uPulse-chase* experiment. **D)** Either whole-cell lysates (Input, left) or immunoprecipitations to increase signal/noise (IP, right) are shown. **E)** Quantifications of (D); $N = 4$ (mean \pm SEM). **F)** Immunoblots of IL-12 α Q57BCNK expression after different time points of the BCNK-excess-induced chase. The same samples as in (D), Input, were used, showing a decrease in the fluorescently labeled IL-12 α Q57BCNK pool and an increase in non-labeled protein levels.

Conclusions

In this study, we have established a minimally invasive approach to monitor protein turnover in cells. To this end we incorporated the tetrazine-reactive amino acid BCNK into different positions of the two human interleukins IL-12 and IL-23. BCNK incorporation was completely compatible with wt-like folding, assembly, cellular quality control, and function of the interleukins. These characteristics allowed us to establish *uChase* as a new assay for monitoring protein degradation in mammalian cells. Our approach does not depend on any tag or other significant modifications of the protein of interest. It is furthermore compatible with different proteins even at very low expression levels, allows rapid degradation processes to be monitored, and does not depend on any downstream enrichment processes (e.g., immunoprecipitation, in which a specific antibody is needed). Furthermore, no global inhibition of translation is needed as in CHX chases; this can have pleiotropic effects and lead, for example, to the unwanted degradation of ERAD factors relevant for the protein under scrutiny. It should be noted that due to the low expression levels of interleukins, background labeling is present; for proteins expressed at higher levels this was mostly absent (Figure S3). Although we monitor protein turnover through in-gel fluorescence, we envision that our approach might be amenable to future microscopy/FACS-based live-cell assays to monitor protein degradation directly in living cells when expression is sufficiently high. This would be a major advantage over currently available approaches. Use of overexpressed proteins, however, of course always comes with the caveat of possibly altered turnover if

important factors become limiting. We show that the technique we have established also provides the basis for more complex fluorescence-based pulse-chase assays. Furthermore, because we were able to confirm receptor binding of our modified interleukins, fluorescently modified interleukins might provide a valuable tool for assessing the characteristics of their receptor engagement and/or to include other chemically reactive probes to modulate their functions selectively and thus go beyond being a tool for measuring protein turnover.

Experimental Section

See the Supporting Information for details on the materials and experimental procedures used, synthesis of small-molecule compounds, and additional figures.

Acknowledgements

Y.G.M. gratefully acknowledges funding from a DAAD PhD scholarship. K.L. and M.J.F. are Rudolf Mößbauer Tenure Track Professors and as such gratefully acknowledge funding through the Marie Curie COFUND program and the Technical University of Munich Institute for Advanced Study, funded by the German Excellence Initiative and the European Union Seventh Framework Program under Grant Agreement 291763. This work was performed within the framework of SFB 1035 (German Research Foundation DFG, Sonderforschungsbereich 1035, projects B10 and B11).

Conflict of Interest

The authors declare no conflict of interest.

Keywords: bio-orthogonal reactions · fluorescent probes · genetic code expansion · interleukins · protein folding

- [1] A. R. Fersht, V. Daggett, *Cell* **2002**, *108*, 573–582.
- [2] F. U. Hartl, M. Hayer-Hartl, *Nat. Struct. Mol. Biol.* **2009**, *16*, 574–581.
- [3] L. M. Luheshi, D. C. Crowther, C. M. Dobson, *Curr. Opin. Chem. Biol.* **2008**, *12*, 25–31.
- [4] B. M. Adams, M. E. Oster, D. N. Hebert, *Protein J.* **2019**, *38*, 317–329.
- [5] L. Ellgaard, N. McCaul, A. Chatsivili, I. Braakman, *Traffic* **2016**, *17*, 615–638.
- [6] I. Braakman, N. J. Balleid, *Annu. Rev. Biochem.* **2011**, *80*, 71–99.
- [7] S. S. Vembar, J. L. Brodsky, *Nat. Rev. Mol. Cell Biol.* **2008**, *9*, 944–957.
- [8] M. H. Smith, H. L. Ploegh, J. S. Weissman, *Science* **2011**, *334*, 1086–1090.
- [9] C. J. Guerriero, J. L. Brodsky, *Physiol. Rev.* **2012**, *92*, 537–576.
- [10] E. Simon, D. Kornitzer, *Methods Enzymol.* **2014**, *536*, 65–75.
- [11] A. Khmelinskii, M. Meurer, C. T. Ho, B. Besenbeck, J. Fuller, M. K. Lemberg, B. Bukau, A. Mogk, M. Knop, *Mol. Biol. Cell* **2016**, *27*, 360–370.
- [12] A. B. Alber, E. R. Paquet, M. Biserni, F. Naef, D. M. Suter, *Mol. Cell* **2018**, *71*, 1079–1091.
- [13] N. Schneider, C. Gabelein, J. Wiener, T. Georgiev, N. Gobet, W. Weber, M. Meier, *ACS Chem. Biol.* **2018**, *13*, 3049–3053.
- [14] S. Mayer, K. Lang, *Synthesis* **2017**, *49*, 830–848.
- [15] B. L. Oliveira, Z. Guo, G. J. L. Bernardes, *Chem. Soc. Rev.* **2017**, *46*, 4895–4950.
- [16] K. Lang, L. Davis, S. Wallace, M. Mahesh, D. J. Cox, M. L. Blackman, J. M. Fox, J. W. Chin, *J. Am. Chem. Soc.* **2012**, *134*, 10317–10320.
- [17] T. Plass, S. Milles, C. Koehler, J. Szymanski, R. Mueller, M. Wiessler, C. Schultz, E. A. Lemke, *Angew. Chem. Int. Ed.* **2012**, *51*, 4166–4170; *Angew. Chem.* **2012**, *124*, 4242–4246.
- [18] A. Borrmann, S. Milles, T. Plass, J. Dommerholt, J. M. Verkade, M. Wiessler, C. Schultz, J. C. van Hest, F. L. van Delft, E. A. Lemke, *ChemBioChem* **2012**, *13*, 2094–2099.
- [19] I. Nikic, T. Plass, O. Schraidt, J. Szymanski, J. A. Briggs, C. Schultz, E. A. Lemke, *Angew. Chem. Int. Ed.* **2014**, *53*, 2245–2249; *Angew. Chem.* **2014**, *126*, 2278–2282.
- [20] C. Uttamapinant, J. D. Howe, K. Lang, V. Beranek, L. Davis, M. Mahesh, N. P. Barry, J. W. Chin, *J. Am. Chem. Soc.* **2015**, *137*, 4602–4605.
- [21] N. Aloush, T. Schwartz, A. I. Konig, S. Cohen, E. Brozgol, B. Tam, D. Nachmias, O. Ben-David, Y. Garini, N. Elia, E. Arbely, *Sci. Rep.* **2018**, *8*, 14527.
- [22] T. Schwartz, N. Aloush, I. Goliand, I. Segal, D. Nachmias, E. Arbely, N. Elia, *Mol. Biol. Cell* **2017**, *28*, 2747–2756.
- [23] R. Serfling, L. Seidel, A. Bock, M. J. Lohse, P. Annibale, I. Coin, *ACS Chem. Biol.* **2019**, *14*, 1141–1149.
- [24] Y. H. Tsai, S. Essig, J. R. James, K. Lang, J. W. Chin, *Nat. Chem.* **2015**, *7*, 554–561.
- [25] D. C. Dieterich, A. J. Link, J. Graumann, D. A. Tirrell, E. M. Schuman, *Proc. Natl. Acad. Sci. USA* **2006**, *103*, 9482–9487.
- [26] P. Wu, M.-X. Lu, X.-t. Cui, H.-Q. Yang, S.-I. Yu, J.-b. Zhu, X.-I. Sun, B. Lu, *Acta Pharmacol. Sin.* **2016**, *37*, 1307.
- [27] I. Fierro-Monti, J. Racle, C. Hernandez, P. Waridel, V. Hatzimanikatis, M. Quadroni, *PLoS One* **2013**, *8*, e80423.
- [28] D. A. Vignali, V. K. Kuchroo, *Nat. Immunol.* **2012**, *13*, 722–728.
- [29] E. D. Tait Wojno, C. A. Hunter, J. S. Stumhofer, *Immunity* **2019**, *50*, 851–870.
- [30] S. Reitberger, P. Haimerl, I. Aschenbrenner, J. Esser von Bieren, M. J. Feige, *J. Biol. Chem.* **2017**, *292*, 8073–8081.
- [31] S. Meier, S. Bohnacker, C. J. Klose, A. Lopez, C. A. Choe, P. W. N. Schmid, N. Bloemeke, F. Ruhrnoss, M. Haslbeck, J. E. Bieren, M. Sattler, P. S. Huang, M. J. Feige, *Nat. Commun.* **2019**, *10*, 4121.
- [32] R. Jalah, M. Rosati, B. Ganneru, G. R. Pilkington, A. Valentin, V. Kulkarni, C. Bergamaschi, B. Chowdhury, G. M. Zhang, R. K. Beach, C. Alicea, K. E. Broderick, N. Y. Sardesai, G. N. Pavlakis, B. K. Felber, *J. Biol. Chem.* **2013**, *288*, 6763–6776.
- [33] S. V. Mayer, A. Murnauer, M.-K. von Wrisberg, M.-L. Jokisch, K. Lang, *Angew. Chem. Int. Ed.* **2019**, *58*, 15876–15882; *Angew. Chem.* **2019**, *131*, 16023–16029.
- [34] C. Yoon, S. C. Johnston, J. Tang, M. Stahl, J. F. Tobin, W. S. Somers, *EMBO J.* **2000**, *19*, 3530–3541.
- [35] B. Oppmann, R. Lesley, B. Blom, J. C. Timans, Y. Xu, B. Hunte, F. Vega, N. Yu, J. Wang, K. Singh, F. Zonin, E. Vaisberg, T. Churakova, M. Liu, D. Gorman, J. Wagner, S. Zurawski, Y. Liu, J. S. Abrams, K. W. Moore, D. Rennick, R. de Waal-Malefyt, C. Hannum, J. F. Bazan, R. A. Kastelein, *Immunity* **2000**, *13*, 715–725.
- [36] P. J. Lupardus, K. C. Garcia, *J. Mol. Biol.* **2008**, *382*, 931–941.
- [37] E. Nadav, A. Shmueli, H. Barr, H. Gonen, A. Ciechanover, Y. Reiss, *Biochem. Biophys. Res. Commun.* **2003**, *303*, 91–97.
- [38] I. Braakman, L. Lamriben, G. van Zadelhoff, D. N. Hebert, *Curr. Protoc. Protein Sci.* **2017**, *90*, 14.1.1–14.1.21.

Manuscript received: October 27, 2019

Revised manuscript received: January 28, 2020

Accepted manuscript online: February 3, 2020

Version of record online: March 9, 2020